PERGAMON

Available online at www.sciencedirect.com

SCIENCE DIRECT®

Polyhedron 22 (2003) 2317–2324

POLYHEDRON

www.elsevier.com/locate/poly

Magnetic and structural characterisation of the layered materials $AMnFe(C_2S_2O_2)_3$

Simon G. Carling [a,*], Justin M. Bradley [a], Dirk Visser [b,c,d], Peter Day [a]

[a] Davy-Faraday Research Laboratory, Royal Institution of Great Britain, 21 Albemarle Street, London W1S 4BS, UK
[b] Department of Physics, Warwick University, Coventry CV4 7AL, NWO-EW UK
[c] ISIS Facility, Rutherford Appleton Laboratory, Chilton, Didcot OX11 0QX, UK
[d] IRI, TU-Delft, Mekelweg 15, 2629JB Delft, The Netherlands

Received 7 October 2002; accepted 11 March 2003

Abstract

We present structural and magnetic data on the series of compounds $AMn^{II}Fe^{III}(C_2S_2O_2)_3$ with $A = N(C_nH_{2n+1})_4$ ($n = 3$–5) or $P(C_6H_5)_4$. The tetra-alkyl ammonium compounds are all ferromagnets with $T_C = 10$ K, whilst the tetraphenyl phosphonium compound is a ferrimagnet with $T_N = 15$ K. EXAFS spectroscopy shows that there is significant disorder in the orientation of the dithio-oxalate moiety, while high resolution X-ray powder diffraction measurements prove that the dithio-oxalate materials are structurally analogous to the layered oxalates.

Keywords: Magnetic and structural characterisation; Layered materials; $AMnFe(C_2S_2O_2)_3$

1. Introduction

Because of their unusual magnetic properties, there has been much interest over recent years in the series of bimetallic tris-oxalato salts with the general formula $A[MM'(C_2O_4)_3]$, where A^+ is an organic cation and M and M′ are, respectively, divalent and trivalent transition metal ions [1–3]. The metal ions, bridged by the ambidentate $C_2O_4^{2-}$ ligand, form hexagonal honeycomb layers interleaved by the organic cations, which fill the spaces in the honeycomb. Analogous dithio-oxalate compounds have also been reported [4–6] with both Cr^{3+} and Fe^{3+} as the trivalent ion and a variety of divalent metal ions. We report here on a series of compounds containing Mn^{2+} and Fe^{3+}.

* Corresponding author. Tel.: +44-20-7409-2992; fax: +44-20-7629-3569.
E-mail address: simon@ri.ac.uk (S.G. Carling).

2. Experimental

2.1. Synthesis

All samples were prepared in a similar fashion to that previously reported by Okawa et al. [4] 0.4 g (1 mmol) of $Fe(NO_3)_3 \cdot 9H_2O$ was dissolved in 25 ml of degassed H_2O. 0.5 g (3 mmol) of di-potassium 1,2-dithio-oxalate was then added and the solution turned the characteristic deep purple colour of $Fe(C_2S_2O_2)_3^{3-}$ (aq). After stirring for 20 min, 1 mmol of $MnSO_4 \cdot 4H_2O$ was added and the solution stirred for further 10 min. The solution was then filtered to remove any precipitated S or FeS, 1 mmol of ABr, where $A = N(C_nH_{2n+1})_4$ ($n = 3$–5) or $P(C_6H_5)_4$, was added and the stirring stopped. The solution was then left to stand until precipitation of $AM^{II}Fe(C_2S_2O_2)_3$ was complete, the product filtered, washed with successive aliquots of water, MeOH and Et_2O and dried under vacuum. Elemental analyses were

0277-5387/03/$ - see front matter © 2003 Elsevier Science Ltd. All rights reserved.
doi:10.1016/S0277-5387(03)00297-3

Table 1
Elemental composition of $AMnFe(C_2S_2O_2)_3$

Sample	Percentage by mass	Element					
		C	H	N/P	S	Mn	Fe
$N(C_3H_7)_4MnFe(C_2S_2O_2)_3$	Calculated	32.88	4.29	2.13	29.17	8.35	8.49
	Observed	31.97	4.34	2.18	27.32	7.36	8.56
$N(C_4H_9)_4MnFe(C_2S_2O_2)_3$	Calculated	37.03	5.08	1.96	26.91	7.70	7.83
	Observed	35.46	5.15	2.07	25.76	7.08	7.99
$N(C_5H_{11})_4MnFe(C_2S_2O_2)_3$	Calculated	40.57	5.76	1.82	24.92	7.14	7.25
	Observed	38.75	5.90	2.01	22.97	6.43	7.49
$P(C_6H_5)_4MnFe(C_2S_2O_2)_3$	Calculated	44.45	2.49	3.82	23.69	6.78	6.90
	Observed	42.75	2.58	3.91	21.48	6.09	7.21

performed by the analytical service of the Chemistry Department of the University of Manchester and are shown in Table 1. In all cases there is a deficiency of both sulfur and carbon. In all cases the sulphur and carbon content observed is lower than the value calculated from the ideal formula. The dithio-oxalate ligand is prone to oxidation and decomposition on prolonged exposure to air. The hydrogen and nitrogen/phosphorous content of the samples are close to the expected values showing that the deficiency in carbon must be due to the dithio-oxalate ligand rather than the organic cation. It seems likely therefore that the deficiencies in sulphur and carbon are caused by decomposition of the dithio-oxalate ligand whilst in transit for analysis.

2.2. Structural characterisation

Powder diffraction profiles were measured on a Siemens D500 diffractometer in reflection geometry. A primary monochromator was used, eliminating all but Cu $K\alpha_1$ radiation. An angular range of 5–45° 2θ was measured with a step size of 0.02°, counting for 20 s per point and using collimation slits limiting the beam divergence to 0.3°. As with the Cr^{3+} compounds reported elsewhere [3], the series $AMnFe(C_2S_2O_2)_3$ were found to crystallise in the hexagonal space group $P6_3$. The stacking motif was found to be A–B with no evidence of a second phase with a six layer repeat or of stacking faults within the crystallites such as have been found in the analogous oxalate compounds [7]. Lattice parameters are reported in Table 2. The increase in interlayer separation is less marked than was found for the series $N(C_nH_{2n+1})_4FeCr(C_2S_2O_2)_3$. Within the series, the area of the ab plane is independent of n in contrast to the analogous oxalate series in which there is an increase in the a parameter with increasing n. The dependence of the increase in interlayer separation on n is identical to that of the chromium compounds with a much greater increase from $n = 3$ to $n = 4$ than from $n = 4$ to $n = 5$. Again this is in stark contrast to the oxalate systems in which the difference n_{even} to n_{odd} is much greater than n_{odd} to n_{even}, probably due to a change in cation conformation.

Table 2
Lattice parameters of (cation) $MnFe(C_2S_2O_2)_3$

Cation (MnFe)	a (Å)	c (Å)
$N(C_3H_7)_4^+$	10.12	16.00
$N(C_4H_9)_4^+$	10.13	18.02
$N(C_5H_{11})_4^+$	10.11	18.14
PPh_4^+	10.19	18.32

2.3. Magnetic characterisation

Bulk magnetization measurements were carried out on polycrystalline samples with a Quantum Design MPMS7 magnetometer. The samples were initially cooled in the absence of an applied field, then measured while warming in a field of 100 Oe. The samples were then recooled in the applied field and remeasured. Plots of χ and $1/\chi$ versus temperature are shown in Fig. 1 and the magnetic parameters determined are given in Table 3. Hysteresis measurements were carried out on $N(C_5H_{11})_4MnFe(C_2S_2O_2)_3$ at 5, 10 and 15 K. This compound was found to be a soft magnet but displayed the largest hysteresis effect of any of the dithio-oxalates studied. The parameters extracted from this data are listed in Table 4. The area of the hysteresis loop is reduced sharply between 5 and 10 K and no hysteresis effect is observed at 15 K ($T > T_c$).

2.4. EXAFS spectroscopy

EXAFS spectra were measured on station 7.1 at the SRS, Daresbury. All measurements were made in transmission mode at room temperature. Two sets of data over a 700 eV range through the absorption edge were summed for each measurement. Spectra were recorded for both the Mn and Fe K_1 absorption edges for each compound. Analyses of the EXAFS spectra

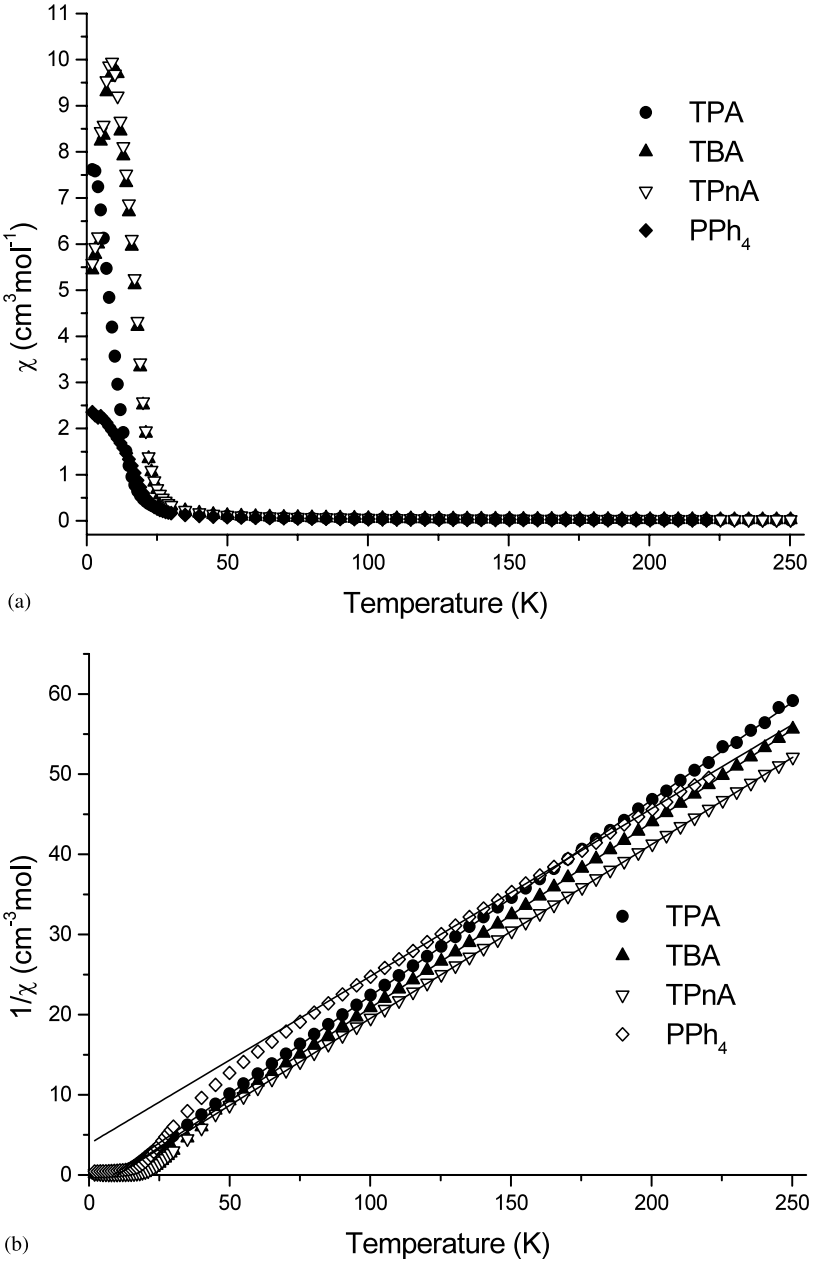

Fig. 1. (a) χ and (b) $1/\chi$ vs. temperature for $AMnFe(C_2S_2O_2)_3$.

Table 3
Parameters for the fits of magnetic data on $AMnFe(C_2S_2O_2)_3$

Cation	T_c (K)	C ($cm^3\ mol^{-1}\ K$)	θ (K)	μ_{eff} (μ_B) (at 300 K)	M_{100} (at 5 K) ($cm^3\ Gmol^{-1}$)
$N(C_3H_7)_4^+$	10	4.10	+10	5.81	+761
$N(C_4H_9)_4^+$	10	4.32	+10	6.63	+544
$N(C_5H_{11})_4^+$	10	4.61	+10	6.67	+558
PPh_4	15	4.82	−20	5.96	+235

were carried out using the standard packages of the Daresbury laboratory. Summation and calibration of the spectra were performed using ExCalib, background subtraction using ExBrook and analysis of the spectra using ExCurv98.

2.5. High resolution X-ray powder diffraction

High resolution X-ray powder diffraction profiles were recorded on $P(C_6H_5)_4$ $MnFe(C_2O_2S_2)_3$ at room temperature on the BM16 diffractometer at the Eur-

Table 4
Hysteresis parameters for $N(C_5H_{11})_4MnFe(C_2O_2S_2)_3$

Temperature (K)	M_{sat} (2T) (μ_{eff} fmu^{-1})	R_M(H→0 +ve) (cm^3 Gmol^{-1})	R_M(H→0 −ve) (cm^3 Gmol^{-1})	$\lvert\Delta R_M\rvert$ (cm^3 Gmol^{-1})
5	1.92	434	−385	819
10	1.81	98	−96	194
15	1.63	–	–	–

Table 5
Bond lengths and temperature factors from the preliminary fits of the EXAFS spectra of $AMn^{II}Fe^{III}(C_2S_2O_2)_3$

Sample and model	r (M–O) (Å)	a (M–O)	r (M–S) (Å)	a (M–S)	R (%)
$N(C_3H_7)_4MnFe(C_2S_2O_2)_3$ **MO_6**	2.16	0.0206	–	–	9.22
$N(C_3H_7)_4MnFe(C_2S_2O_2)_3$ **MO_4S_2**	2.14	0.0208	2.34	0.0208	8.59
$N(C_4H_9)_4MnFe(C_2S_2O_2)_3$ **MO_6**	2.056	0.0850	–	–	7.64
$N(C_4H_9)_4MnFe(C_2S_2O_2)_3$ **MO_4S_2**	2.12	0.0205	2.36	0.0205	7.72
$N(C_3H_7)_4MnFe(C_2S_2O_2)_3$ **MS_6**	–	–	–	–	–
$N(C_3H_7)_4MnFe(C_2S_2O_2)_3$ **MS_4O_2**	2.073	0.1129	2.25	0.0121	2.92
$N(C_4H_9)_4MnFe(C_2S_2O_2)_3$ **MS_6**	–	–	2.25	0.0220	9.85
$N(C_4H_9)_4MnFe(C_2S_2O_2)_3$ **MS_4O_2**	2.12	0.016	2.26	0.016	6.342

Bold face indicates the absorption edge.

opean Synchrotron Radiation Facility, Grenoble. A wavelength of 0.80312 Å was used. The sample was mounted in a 0.7 mm glass capillary and diffraction profiles were recorded between −4 and 38° 2θ at a scan rate of 0.6° min^{-1}. Five profiles were summed and binned to a step size of 0.003°.

3. Results and discussion

3.1. Magnetic behaviour

In all cases, the observed effective magnetic moments are close to the expected values for high-spin Mn^{2+} ($S = 5/2$) and low-spin Fe^{3+} ($S = 1/2$). This observation suggests that the trivalent metal is co-ordinated by six sulfur atoms, since Fe^{3+} in an oxygen environment would be expected to be high-spin. The three tetra-alkyl ammonium compounds all show ferromagnetic Curie–Weiss behaviour and order at 10 K. The tetraphenyl phosphonium salt, however, is ferrimagnetic with an ordering temperature of 15 K.

3.2. Metal ion coordination

As expected, the EXAFS spectra show that the local environment of the metal atoms is similar in all of the materials studied. Only the first shell of the EXAFS data was fitted in order to model the nearest neighbors of the central metal and refine the ratio of oxygen to sulfur. Initial analysis showed that the degree of ligand disorder in the freshly prepared samples studied was relatively low. Thus the models chosen for refinement were first shells containing O_6 and O_4S_2 for M^{II} and containing S_6 and S_4O_2 for M^{III}. Initial bond lengths and angles for the refinements were calculated using crystallographic data from $N(C_5H_{11})_4MnFe(C_2O_4)_3$ [8] and $[Ni(phen)_3][NaCo(C_2S_2O_2)_3]\cdot C_3H_6O$ [9]. Neither model refines to a satisfactory minimum when fitted individually which is unsurprising since the materials would be expected to contain both environments at low levels of ligand disorder. The individual clusters were refined initially in order to calculate the starting point for a two cluster refinement in which the relative occupancies of the $M^{II}O_6$:$M^{II}O_4S_2$ and $M^{III}S_6$:$M^{III}S_4O_2$ sites were refined, along with bond lengths and thermal parameters.

Table 5 lists the bond lengths, r, and Debye–Waller factors, a, extracted from the single cluster refinements. The bond lengths compare favorably with the crystallographic values and are internally consistent but the Debye–Waller factors are large due to the failure to model the disorder in the first co-ordination shell of the metal. Fig. 2 shows examples of the single cluster fits for the Mn K edge in $N(C_4H_9)_4MnFe(C_2S_2O_2)_3$.

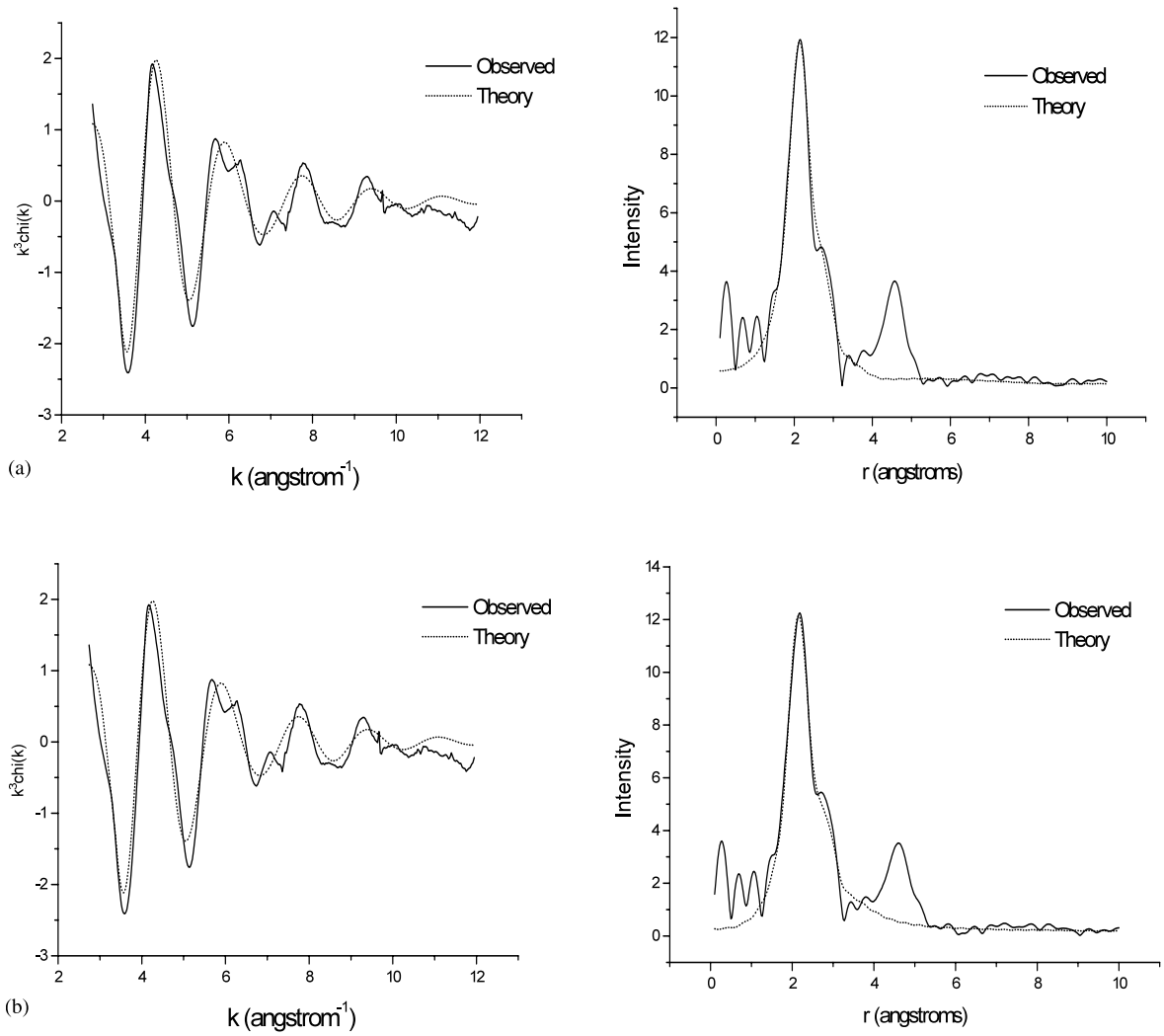

Fig. 2. EXAFS signal and the Fourier transform for the Mn K edge of $N(C_4H_9)_4MnFe(C_2S_2O_2)_3$ fitted to: (a) MnO_6 clusters; and (b) MnO_4S_2 clusters. In each case only the first coordination shell was refined.

The bond lengths and temperature factors of the original single cluster models were allowed to refine in the two cluster models but constrained to be equal for identical metal–ligand linkages. The bond lengths, temperature factors and ratio of ordered to disordered clusters were refined simultaneously. Table 6 lists the results of the two cluster refinements. The order parameter is the percentage of the clusters which are of the ordered MO_6 or MS_6 type.

Extension of the model to two clusters has little effect on the bond lengths, which are consistent with the values determined from crystallography, but leads to a decrease in the thermal parameters as the disorder in the system is taken into account. The amount of disorder in the materials is consistent at both metal edges within the same sample. Fig. 3 shows the EXAFS and Fourier transform of the EXAFS fitted to the two cluster model for $N(C_3H_7)_4MnFe(C_2S_2O_2)_3$.

3.3. Structure refinement

The data taken on BM16 was indexed in spacegroup $P6_3$. Inspection of the symmetries of the special sites in this group showed that the metal ions should be placed on the threefold axes 1/3, 2/3, z and 2/3, 1/3, z respectively, whilst the phosphorus of the tetraphenyl phosphonium ion should be on the 0, 0, z axis. In this way, the chiral nature of the metal ion coordination could be accomodated. Owing to the relatively poor crystallinity of the dithio-oxalate compounds, it was necessary to geometrically constrain the tetraphenyl phosphonium ion. All phenyl rings were constrained to be planar with C–C distances of 1.38 Å and bond angles of 120°. Additionally, the P–C bonds were constrained to be 1.79 Å and the coordination of the phosphorus atom was constrained to be a regular tetrahedron with one P–C bond along the 0, 0, z threefold axis. The isotropic

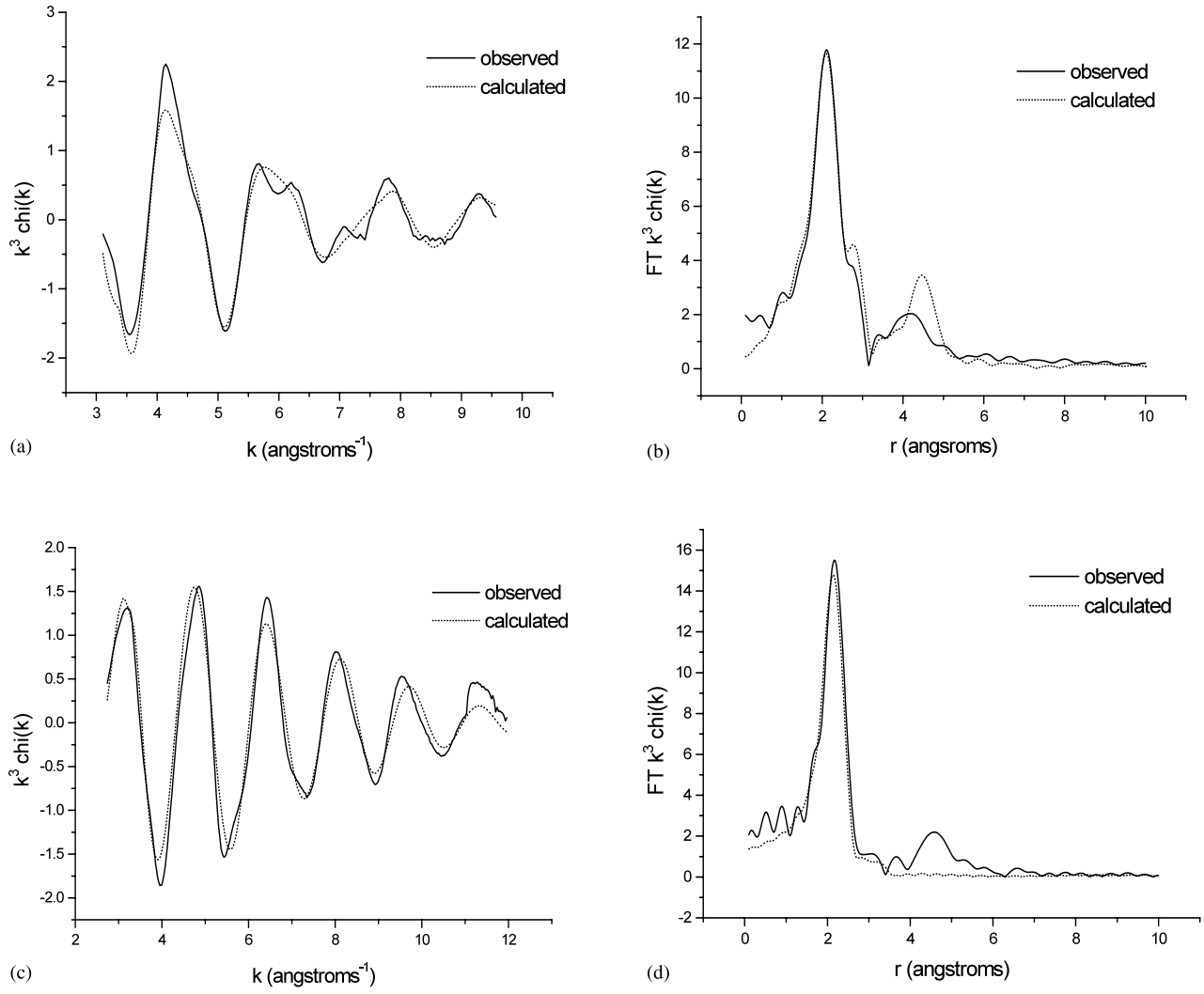

Fig. 3. Two cluster fits of the EXAFS and Fourier transform of the EXAFS of the manganese (a) and (b) and iron (c) and (d) edges of $N(C_3H_7)_4MnFe(C_2S_2O_2)_3$. In each case only the first coordination shell was refined.

temperature factors of all phenyl-ring carbons were constrained to remain equal, as were those of similar atoms in the dithio-oxalate group. The dithio-oxalate group was placed such that the Mn–O and Fe–S bonds were compatible with the EXAFS results described above. A small impurity phase was identified as S_8 and its lattice parameters and peak shape were refined simultaneously with the major phase. Refinement using the GSAS package [10] led to a final structure with $R_{wp} = 6.06$ and $R_p = 4.76\%$. The resulting profiles are shown in Fig. 4 and Table 7 gives the atomic parameters. The metal-containing layer of the structure is shown in Fig. 5, from which the tetraphenyl phosphonium cation has been omitted for clarity.

The refined unit cell parameters are $a = 10.1560(3)$ and $c = 18.3604(9)$ Å. The metal ions are each coordinated by three short and three long bonds, with Mn–O distances of 1.861(21) and 2.180(20) Å and Fe–S distances of 2.272(22) and 2.616(15) Å. It is clear from Table 6 that the dithio-oxalate group has not refined well, having unphysical values for U_{iso} as well as a severely distorted geometry. This is consistent with the EXAFS results indicating disorder in the orientation of the anion. The very high values of U_{iso} found for the sulfur atoms and the negative values found for the oxygen atoms are precisely what would be expected if some Fe^{3+} are partially coordinated by oxygen and some Mn^{2+} by sulfur.

4. Conclusions

The compounds $AMnFe(C_2S_2O_2)_3$ have been shown to adopt similar honeycomb layered structures to those

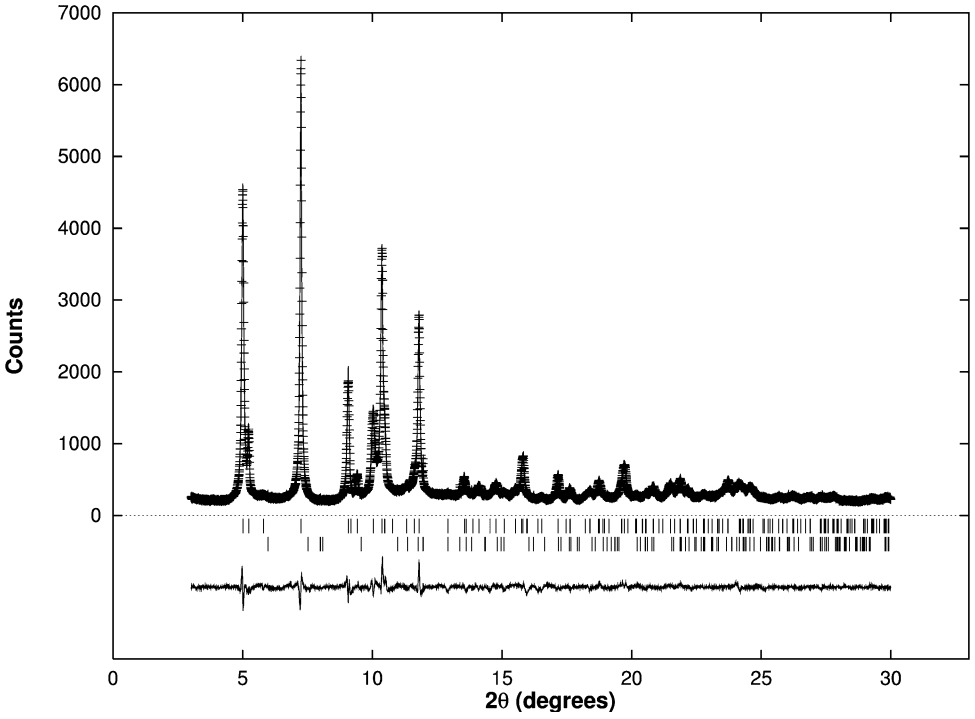

Fig. 4. Observed (crosses), calculated (upper full line) and difference profiles of the Rietveld refinement of $P(C_6H_5)_4MnFe(C_2S_2O_2)_3$. Vertical bars indicate reflection positions for the main phase (upper) and S_8 impurity phase (lower).

Table 6
Refined parameters from the two cluster models of EXAFS data on $AMn^{II}Fe^{III}(C_2S_2O_2)$

Sample	*R* M–O (Å)	*a* M–O	*r* M–S (Å)	*a* M–S	Order (%)	*R* (%)
$N(C_3H_7)_4MnFe(C_2S_2O_2)_3$	2.18	0.017	2.37	0.016	25.6	6.74
$N(C_3H_7)_4MnFe(C_2S_2O_2)_3$	2.17	0.034	2.25	0.014	26.7	2.71
$N(C_4H_9)_4MnFe(C_2S_2O_2)_3$	2.16	0.013	2.38	0.056	30.8	3.41
$N(C_4H_9)_4MnFe(C_2S_2O_2)_3$	2.10	0.031	2.25	0.020	31.2	3.71

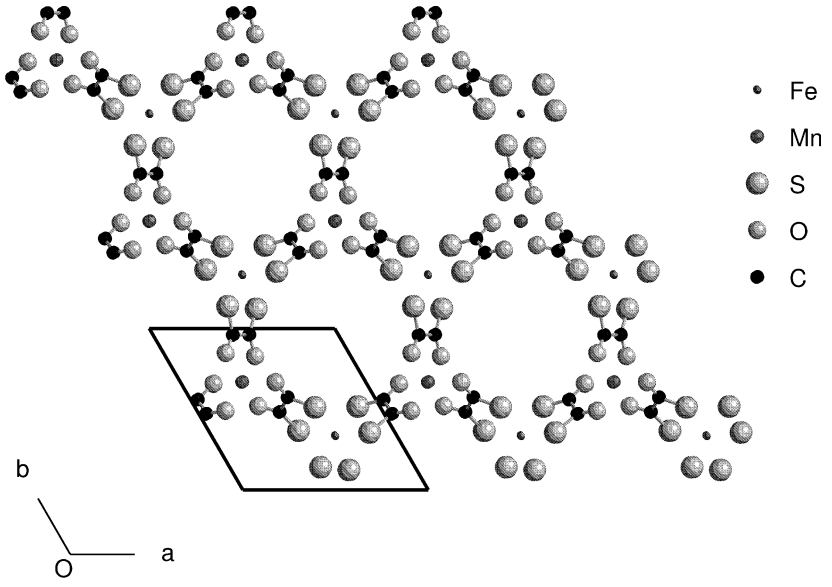

Fig. 5. Metal dithio-oxalate layer of $P(C_6H_5)_4MnFe(C_2S_2O_2)_3$ viewed along [001]. The organic cation has been omitted for clarity.

Table 7
Atomic parameters of the structural refinement of $P(C_6H_5)_4MnFe(C_2S_2O_2)_3$

Atom	*X*	*y*	*z*	Fract	$100 \times U_{iso}$
Mn	1/3	2/3	0.2456(7)	1	6.45(52)
Fe	2/3	1/3	0.2444(7)	1	6.55(60)
O1	0.478(2)	0.676(3)	0.3105(9)	1	−2.13(42)
C1	0.555(4)	0.657(5)	0.324(2)	1	1.74(138)
S1	0.657(3)	0.507(2)	0.319(1)	1	20.44(74)
O2	0.362(2)	0.506(2)	0.178(1)	1	−2.13(42)
C2	0.545(4)	0.559(4)	0.261(2)	1	1.74(138)
S2	0.480(2)	0.364(2)	0.157(1)	1	20.45(74)
P	0	0	0.5708(6)	1	4.27(50)
C11	0	0	0.6681(6)	1	8.20(50)
C12	0.1177(1)	0.0003(2)	0.7057(7)	1/3	–
C13	0.1212(25)	0.0073(55)	0.7808(7)	1/3	–
C14	0	0	0.8184(7)	1	–
C15	−0.1177(1)	0.0000(2)	0.7808(7)	1/3	–
C16	−0.1176(2)	0.0001(2)	0.7057(7)	1/3	–
C31	−0.1657(1)	0.0002(1)	0.5383(6)	1	–
C32	−0.1789(26)	0.1239(20)	0.5590(17)	1	–
C33	−0.3188(26)	0.1115(24)	0.5460(21)	1	–
C34	−0.4352(19)	−0.0071(36)	0.5082(17)	1	–
C35	−0.4026(14)	−0.1139(21)	−0.4803(19)	1	–
C36	−0.2763(17)	−0.1233(16)	0.5004(13)	1	–

found in the analogous oxalate compounds. The sulfur atoms of the dithio-oxalate anion predominantly coordinate to the Fe^{3+} ion, but at some sites one anion is reversed. As has been found in the oxalates $AFe^{II}Fe^{III}(C_2O_4)_3$, a seemingly trivial change in the organic cation A results in a drastic change in magnetic behaviour; in this case compounds with tetra-alkyl ammonium cations show ferromagnetic exchange whilst the tetraphenyl phosphonium compound shows antiferromagnetic exchange.

References

[1] H. Tamazaki, Z. Zhong, N. Matsumoto, S. Kida, M. Koikawa, N. Aihiwa, Y. Hashimoto, H. Okawa, J. Am. Chem. Soc. 114 (1992) 6974.
[2] S. Decurtins, H.W. Schmalle, R. Oswald, A. Linden, J. Ensling, P. Gütlich, A. Hauser, Inorg. Chim. Acta 216 (1994) 65.
[3] C. Mathonière, C.J. Nuttall, S.G. Carling, P. Day, Inorg. Chem. 35 (1996) 1201.
[4] H. Okawa, M. Mitsumi, M. Ohba, M. Kodera, N. Matsumoto, Bull. Chem. Soc. Jpn. 67 (1994) 2139.
[5] N. Kojima, W. Aoki, M. Itoi, Y. Ono, M. Seto, Y. Kobayashi, Yu. Maeda, Solid State Commu. 120 (2001) 165.
[6] J.M. Bradley, S.G. Carling, D. Visser, D. Hautot, P. Day, G.J. Long, Inorg. Chem. 2002, in press.
[7] C.J. Nuttall, P. Day, Solid State Commu. 110 (1999) 39.
[8] S.G. Carling, C. Mathonière, P. Day, K. Malik, S. Coles, M. Hursthouse, J. Chem. Soc. Dalton Trans. (1996) 1839.
[9] S. Decurtins, H. Schmalle, R. Pellaux, P. Schneuwly, A. Hauser, Inorg. Chem. 35 (1996) 1451.
[10] A.C. Larson, R.B. Von Dreele, LANL Report, LAUR 86–748, 1986.